

# Mechanistic Study on C–C Bond Formation of a Nickel(I) Monocarbonyl Species with Alkyl Iodides: Experimental and Computational Investigations

Changho Yoo,<sup>†</sup> Manjaly J. Ajitha,<sup>‡</sup> Yousung Jung,<sup>\*,†,‡</sup> and Yunho Lee<sup>\*,†</sup>

<sup>†</sup>Department of Chemistry and <sup>‡</sup>Graduate School of EEWS, Korea Advanced Institute of Science and Technology, Daejeon 305-701, Republic of Korea

## Supporting Information

**ABSTRACT:** An open-shell reaction of the nickel(I) carbonyl species (PNP)Ni-CO (**1**) with iodoalkanes has been explored experimentally and theoretically. The initial iodine radical abstraction by a nickel(I) carbonyl species was suggested to produce (PNP)Ni-I (**4**) and the concomitant alkyl radical, according to a series of experimental indications involving stoichiometric controls employing iodoalkanes. Corresponding alkyl radical generation was also confirmed by radical trapping experiments using Gomberg's dimer. Molecular modeling supports that the nickel acyl species (PNP)Ni-COCH<sub>3</sub> (**2**) can be formed by a direct C–C bond formation between a carbonyl ligand of **1** and a methyl radical. As an alternative pathway, the five-coordinate intermediate species (PNP)Ni(CO)(CH<sub>3</sub>) (**5**) that involves both CO and CH<sub>3</sub> binding at a nickel(II) center is also suggested with a comparable activation barrier, although this pathway energetically favors the formation of (PNP)Ni-CH<sub>3</sub> (**3**) via a barrierless elimination of CO over a CO migratory insertion. Thus, our present work supports that the direct C–C bond coupling occurs between an alkyl radical and the carbonyl ligand at a monovalent nickel center in the generation of an acyl product.

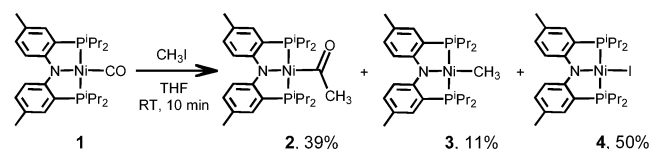


## INTRODUCTION

Monovalent nickel chemistry is drawing much attention in both organometallic and bioorganometallic chemistry.<sup>1–3</sup> With aryl and alkyl halides, the nickel(I/III) mechanism was recently proposed for nickel-catalyzed cross-coupling reactions, distinctive from a well-known Ni(0) to Ni(II) cycle.<sup>2</sup> Carbon monoxide activation mediated by nickel(I) is also crucial in the reaction of the biological acetyl-CoA synthase (ACS), in which a nickel(I) carbonyl species is proposed as an active intermediate according to the paramagnetic mechanism.<sup>3</sup> Although an open-shell nickel(I) carbonyl intermediate was proposed in this C–C bond formation, its reactivity is currently unexplored. While a radical carbonylation of free CO with an alkyl radical is well established,<sup>4</sup> the open-shell C–C bond formation of transition-metal-coordinated CO is uncommon.<sup>5</sup>

We have recently reported the reaction of a nickel(I) carbonyl complex (PNP)Ni-CO (**1**) supported by a PNP ligand (PNP<sup>−</sup> = N[2-PiPr<sub>2</sub>-4-Me-C<sub>6</sub>H<sub>3</sub>]<sub>2</sub><sup>−</sup>) with iodomethane, revealing the formation of the nickel(II) acetyl species (PNP)Ni-COCH<sub>3</sub> (**2**) along with (PNP)Ni-CH<sub>3</sub> (**3**) and (PNP)Ni-I (**4**) (Scheme 1).<sup>6</sup> We postulated that a nickel(I) carbonyl species initiates the reaction through iodine radical abstraction with the concomitant formation of a corresponding methyl radical. This reaction is evocative of C–X bond activation mediated by nickel(I) species; such transformations are proposed in nickel cross-coupling reactions.<sup>2,7</sup> The initial C–X bond activation mediated by nickel(I) was corroborated with nickel(I) complexes supported by pyridine-based ligands.<sup>7</sup> According to electron paramagnetic resonance (EPR) spectro-

## Scheme 1

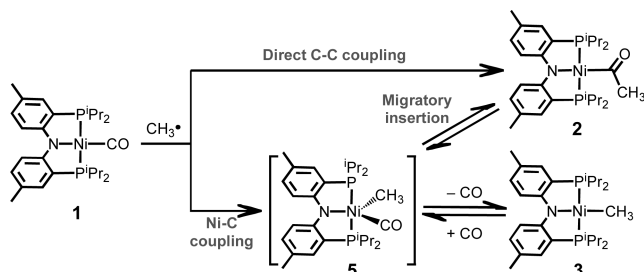


scopic analysis and density functional theory (DFT) studies, those redox processes involved in the reaction originate not from a metal center but from noninnocent ligands. Thus, the alkyl radical formation in those systems occurs via a ligand-based electron transfer process.<sup>7a,c,d</sup> To date, reports of reactions involving genuine nickel(I) species with alkyl halide are fairly limited.<sup>8</sup>

In addition, the formation of two methylated products, (PNP)Ni-COCH<sub>3</sub> (**2**) and (PNP)Ni-CH<sub>3</sub> (**3**), raises a question regarding their reaction pathways. The five-coordinate alkyl metal carbonyl species (PNP)Ni(CO)(CH<sub>3</sub>) (**5**) can be anticipated as a reaction intermediate (Scheme 2). However, we cannot rule out direct C–C bond formation between a methyl radical and a CO ligand in the formation of a nickel acetyl species (Scheme 2). While direct alkylation at a coordinated CO was recently proposed, there have been only a few literature precedents.<sup>5,9</sup>

Received: June 23, 2015

Scheme 2



Herein, we report the detailed reaction mechanism of (PNP)Ni-CO (**1**) with iodoalkanes on the basis of both experimental and theoretical investigations. The initial alkyl radical generation was demonstrated by stoichiometric control experiments and resulting product analysis, which were well supported by the results of DFT calculations. The alkyl radical generation was further confirmed by radical trapping experiments. Theoretical evaluations on both the methylated products (PNP)Ni-COCH<sub>3</sub> (**2**) and (PNP)Ni-CH<sub>3</sub> (**3**) and the possible five-coordinate intermediate (PNP)Ni(CO)(Me) (**5**) suggest that a direct C–C bond formation occurs between a methyl radical and a coordinated CO ligand.

## RESULTS AND DISCUSSION

We recently reported nickel(II/I/0) monocarbonyl species supported by an anionic tridentate PNP ligand and their reactivity toward iodoalkanes.<sup>6</sup> While the divalent nickel monocarbonyl species {(PNP)Ni-CO}{BF<sub>4</sub>} does not show any reactivity toward MeI, the zerovalent congener (PNP)-Ni<sup>0</sup>(CO)Na undergoes oxidative addition and CO elimination, resulting in the formation of a nickel(II) methyl species.<sup>6a</sup> Interestingly, (PNP)Ni-CO (**1**) reveals its unique capability to produce a nickel(II) acetyl species via C–C bond coupling, according to the reaction product distribution: Ni-COCH<sub>3</sub> (**2**), 39%; Ni-CH<sub>3</sub> (**3**), 11%; Ni-I (**4**), 50% (Scheme 1). This is comparable to those of reactions with corresponding zerovalent and divalent congeners. In fact, the closed-shell reaction of **1** with MeOTf (OTf = trifluoromethanesulfonate) results in no product formation. Therefore, the corresponding acyl formation at the monovalent nickel center presumably occurs through a radical pathway, rather than the typical S<sub>N</sub>2 type reaction.<sup>6a</sup>

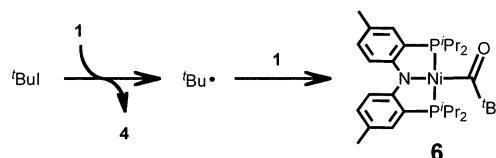
At the initial stage of a radical pathway occurring at a monovalent nickel center, two possible routes can be suggested: initial iodine radical abstraction by nickel(I) followed by concomitant generation of an alkyl radical and initial alkyl radical abstraction with iodine radical generation. To evaluate these two routes and the role of a monovalent nickel ion, we have pursued both experimental and theoretical investigations involving the reaction of alkyl iodides. Since the reaction of (PNP)Ni-CO (**1**) with 1 equiv of *tert*-butyl iodide reveals the formation of (PNP)Ni-I (**4**; 53%) and (PNP)Ni-CO<sup>*t*</sup>Bu (**6**; 47%) (Table 1), iodine radical abstraction might be favorable over *tert*-butyl radical abstraction due to its steric effect. In order to test this hypothesis, we have conducted the same reaction using excess alkyl iodides, where the exclusive production of **4** is expected. To a THF solution of <sup>*t*</sup>BuI (100 equiv) was added a dark green solution of **1** at room temperature, resulting in an immediate color change to yellow, revealing the higher yield of the formation of **4** (73%) (Table 1 and the Experimental Section). This result indicates that the

Table 1. Reaction of (PNP)Ni-CO (**1**) with Alkyl Iodides<sup>10</sup>

RI	amt (equiv)	yield (%)		
		Ni-I ( <b>4</b> )	Ni-COR	Ni-R
<sup><i>t</i></sup> BuI	1	53	47	
<sup><i>t</i></sup> BuI	100	73	27	
MeI	1	50	39	11
MeI	100	50	39	11
CF <sub>3</sub> I	25	64	18 <sup>11</sup>	19

reaction dominantly favors iodine radical abstraction at the first stage followed by the production of **6** via radical coupling between **1** and a *tert*-butyl radical (Scheme 3). The generation

Scheme 3



of **6** (27%), even with a large excess of <sup>*t*</sup>BuI, suggests that the radical coupling reaction between a *tert*-butyl radical and a carbonyl ligand of **1** is more rapid than either (i) the dimerization of *tert*-butyl radicals or (ii) the reaction of **1** with <sup>*t*</sup>BuI.

According to our DFT calculations, the activation barrier ( $\Delta G^\ddagger$ , the energy difference between the transition state and the corresponding prereaction complex) for the formation of (PNP)Ni-I (**4**) by the homolytic cleavage of *tert*-butyl iodide (via TS<sub>1<sup>*t*</sup>Bu</sub>) is 12.3 kcal/mol, whereas that of (PNP)Ni-CO<sup>*t*</sup>Bu (**6**) (via TS<sub>2<sup>*t*</sup>Bu</sub>) is 19.2 kcal/mol (Figure 1). The lower

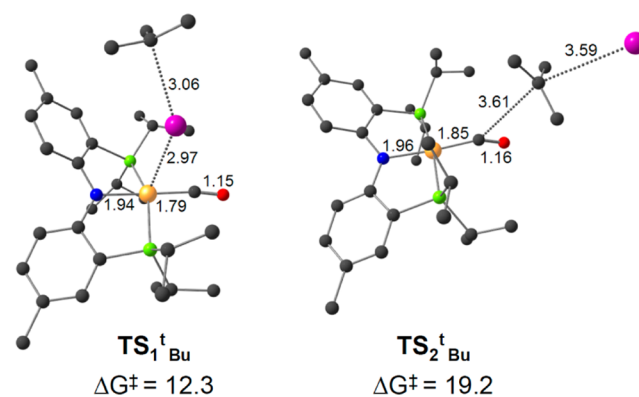


Figure 1. Optimized geometries of the two transition states TS<sub>1<sup>*t*</sup>Bu</sub> and TS<sub>2<sup>*t*</sup>Bu</sub>. Distances are given in Å.  $\Delta G^\ddagger$  values are given in kcal/mol. Color code: black, C; blue, N; green, P; yellow, Ni; pink, I; red, O. Hydrogen atoms are omitted for clarity.

activation barrier of TS<sub>1<sup>*t*</sup>Bu</sub> in comparison to that of TS<sub>2<sup>*t*</sup>Bu</sub> indicates that the formation of **4** occurs prior to the *tert*-butyl radical abstraction, in agreement with the experimental observation. The calculated spin density of **1** indicates a 67% contribution at a nickel center; most of the remaining amount is equally shared between the atoms directly attached to a nickel center (Supporting Information). In TS<sub>1<sup>*t*</sup>Bu</sub> however, the spin density was dramatically decreased at the metal center (21%) with a significant increment of the *tert*-butyl radical character (75%). The five-coordinate intermediate species

(PNP)Ni(CO)(I), formed from the initial iodine radical abstraction, undergoes a fast CO elimination reaction to yield **4**. In the case of the second reaction pathway, since  $\text{TS}_{2\text{tBu}}$  possessing a direct C–C bond interaction between a CO ligand and *tert*-butyl iodide requires  $\sim 7$  kcal/mol higher energy than  $\text{TS}_{1\text{tBu}}$ , the slower reaction is expected. Direct coupling of the *tert*-butyl radical with a nickel center may also be considered as an alternative pathway, but calculation of this species (PNP)Ni(CO)(<sup>t</sup>Bu) was not able to be carried out and always yielded **6**, presumably due to the steric bulkiness of a *tert*-butyl group.

To compare the result obtained from the reaction of (PNP)Ni–CO (**1**) with <sup>t</sup>BuI, we also pursued studies with methyl iodide. The different alkyl radical species (methyl vs *tert*-butyl) impart a steric factor that might affect the reaction pathway. In order to discriminate between the two different reaction routes, iodine radical abstraction vs methyl radical abstraction, we conducted the same experimental and theoretical evaluations on the reaction of (PNP)Ni–CO (**1**) and MeI. Unlike the reactions with <sup>t</sup>BuI, the yields of (PNP)Ni–I (**4**) consistently stood at  $\sim 50\%$  from the reactions of (PNP)Ni–CO (**1**) with both stoichiometric and excess (100 equiv) amounts of MeI (Table 1 and the Experimental Section). This might be due to the instability of a methyl radical, resulting in an instant radical coupling reaction with **1**. To evaluate the electronic consequence with a minimum steric effect, an electron-deficient methyl iodide was utilized. The reaction of **1** with CF<sub>3</sub>I (25 equiv) resulted in the increased formation of **4** (64% yield) (Table 1 and the Experimental Section), suggesting the effect of a relatively stable CF<sub>3</sub> radical.<sup>11</sup>

Since the generation of an iodide radical still cannot be excluded through this additional experimental evidence, we also conducted DFT calculations on the reaction of (PNP)Ni–CO (**1**) with MeI. Similar to the result of the reaction with <sup>t</sup>BuI, the iodine radical abstraction via the homolytic cleavage of MeI also occurs with a lower activation barrier (11.6 kcal/mol) via  $\text{TS}_{1\text{Me}}$  in comparison to that for  $\text{TS}_{2\text{Me}}$  ( $\Delta G^\ddagger = 16.0$  kcal/mol), in which the carbonyl carbon of **1** is found to directly interact with the carbon atom of MeI (Figure 2, vide infra). In  $\text{TS}_{1\text{Me}}$ , 98% of the spin density occurs at a departing methyl moiety, confirming the radical nature of a leaving CH<sub>3</sub> group. Therefore, the theoretical evaluation also suggests that iodine radical abstraction occurs prior to methyl radical generation.

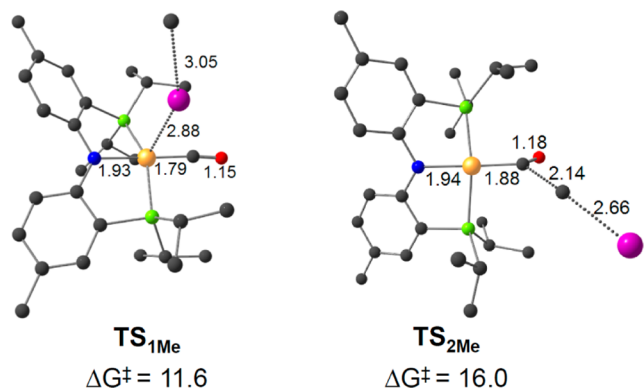


**Figure 2.** Optimized geometries of the two transition states  $\text{TS}_{1\text{Me}}$  and  $\text{TS}_{2\text{Me}}$ . Distances are given in Å.  $\Delta G^\ddagger$  values are given in kcal/mol. Color code: black, C; blue, N; green, P; yellow, Ni; pink, I; red, O. Hydrogen atoms are omitted for clarity.

However, the energy difference between iodine radical vs methyl radical abstraction is smaller (4.4 kcal/mol) than that found in the *tert*-butyl case (6.9 kcal/mol) due to the relative stability of the two organic radicals.

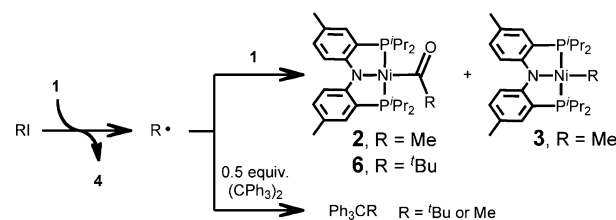
In order to provide evidence for the initial alkyl radical generation, we attempted to trap a radical species by employing Gomberg's dimer,  $(\text{CPh}_3)_2$ , in which a trityl radical ( $\text{Ph}_3\text{C}^\bullet$ ) can be generated by equilibrium dissociation of the dimer in the solution state.<sup>12</sup> In the presence of Gomberg's dimer, (PNP)Ni–CO (**1**) was treated with <sup>t</sup>BuI, revealing dramatic changes in the product formation: 91% of **4** and 9% of **6** (Table 2 and the Experimental Section). Control experiments

**Table 2.** Reaction of (PNP)Ni–CO (**1**) with 1 Equiv of Alkyl Iodides in the Presence of Gomberg's Dimer

RI	amt of $(\text{CPh}_3)_2$ (equiv)	temp (°C)	yield (%)		
			Ni–I ( <b>4</b> )	Ni–COR	Ni–R
<sup>t</sup> BuI	0.5	room temp	91	9	
MeI	0.5	room temp	60	30	10
MeI	0.5	–35	60	29	11
MeI	5	room temp	77	17	6

confirmed that Gomberg's dimer does not react with **1**, <sup>t</sup>BuI, or MeI under the same reaction conditions. It seems that the *tert*-butyl radical was trapped by a trityl radical, resulting in the formation of  $\text{Ph}_3\text{C}^\bullet\text{Bu}$  rather than reaction with **1** (Scheme 4). The identity of  $\text{Ph}_3\text{C}^\bullet\text{Bu}$  isolated via silica gel column chromatography (38% yield) (see the Experimental Section) was confirmed by <sup>1</sup>H NMR spectroscopic data.

**Scheme 4**



To confirm the existence of the corresponding methyl radical generation, the reaction of (PNP)Ni–CO (**1**) with MeI was also conducted in the presence of Gomberg's dimer. To a mixture of **1** and 0.5 equiv of  $(\text{CPh}_3)_2$  (pentane) was added 1 equiv of MeI, and the mixture was stirred for 10 min at room temperature. The resulting solution possessed three species, (PNP)Ni–COCH<sub>3</sub> (**2**; 30%), (PNP)Ni–CH<sub>3</sub> (**3**; 10%), and (PNP)Ni–I (**4**; 60%); the corresponding yields were established by <sup>1</sup>H and <sup>31</sup>P NMR data (Table 2). The effect of Gomberg's dimer was not as significant as the case of the <sup>t</sup>BuI reaction, presumably due to the instability of a methyl radical. Reducing the reaction temperature (–35 °C) turned out to give insignificant trapping of a methyl radical. However, in the presence of 5 equiv of Gomberg's dimer, the yield of **4** increased to 77% (Table 2 and the Experimental Section).  $\text{Ph}_3\text{CMe}$  was isolated by column chromatography in 32% yield, and its identity was confirmed by <sup>1</sup>H NMR analysis. The results obtained from the radical trapping experiments with Gomberg's dimer clearly reveal the preference of initial methyl radical generation over iodine radical production.

The nickel(I)-mediated alkyl radical generation from iodoalkane was initially proposed for the mechanism of

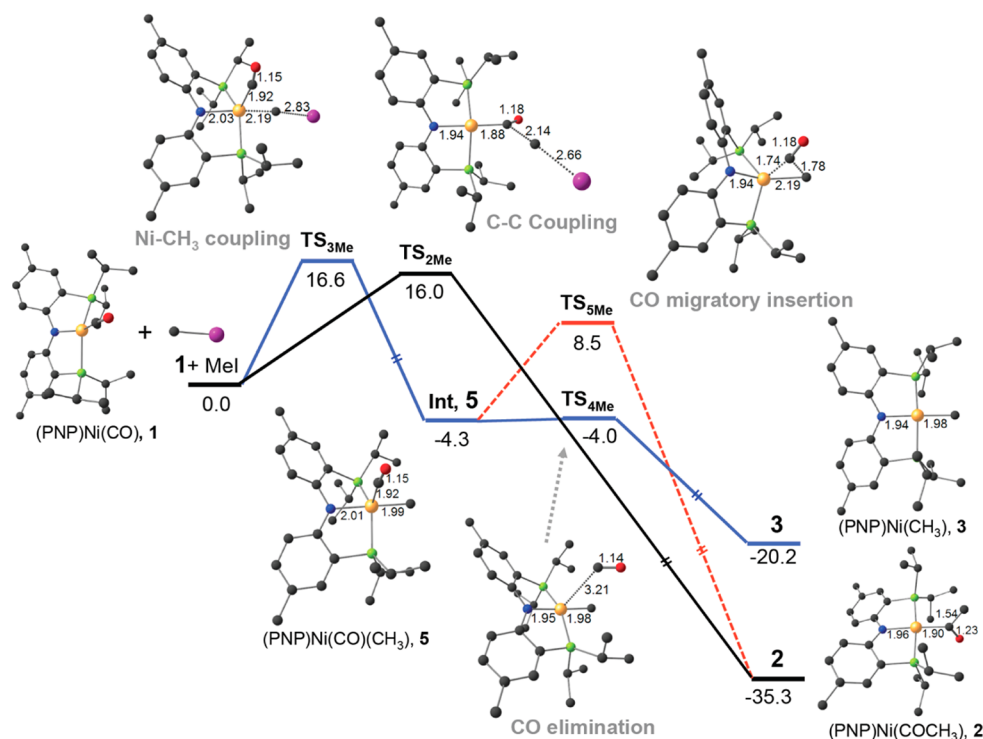


**Figure 3.** Free energy (kcal/mol) profiles of different pathways from (PNP)Ni-CO (**1**) via direct Ni–C bond coupling toward the formation of (PNP)Ni-COCH<sub>3</sub> (**2**) and (PNP)Ni-CH<sub>3</sub> (**3**) through the five-coordinate intermediate (PNP)Ni(CO)(CH<sub>3</sub>) (int, **5**) and via direct C–C bond coupling as an alternative route to produce **2**. Distances are given in Å. Color code: black, C; blue, N; green, P; yellow, Ni; pink, I; red, O. Hydrogen atoms are omitted for clarity.

nickel-catalyzed cross-coupling reactions.<sup>2,7</sup> Vicic and co-workers isolated the nickel(I) methyl species (typ)Ni(CH<sub>3</sub>) with a terpyridine ligand and examined its reaction with cyclohexyl iodide. The formation of a corresponding monoiodo nickel(I) complex with methylcyclohexane suggested the nickel(I)-mediated reaction pathway.<sup>7c</sup> Cárdenas and co-workers conducted the nickel-catalyzed cross-coupling reaction of iodoalkanes with alkyl zinc halides utilizing a pybox-type ligand. In fact, the coupling reactions of several radical clocks, revealing the cyclization/ring opening of unsaturated/cyclic alkyl iodides, indicate the existence of an alkyl radical as a reaction intermediate.<sup>7c</sup> However, a series of EPR and DFT studies suggest that the unpaired electron is located on the ligand, not the metal center.<sup>7a,c,d</sup> Thus, the alkyl radical formation by a nickel(I) species supported by a pyridine-based ligand occurs substantially via a ligand-based electron transfer reaction.<sup>7c,d</sup> According to our previous experiments, the monovalent nickel carbonyl species (PNP)Ni-CO (**1**) possessing significant spin density on a nickel center at 71.2%, exhibits a Ni<sup>I/II</sup> couple at  $-1.23$  V vs Fc/Fc<sup>+</sup>.<sup>6a</sup> The redox properties of **1** cannot reduce methyl iodide via electron transfer.<sup>13</sup> Thus, iodine radical abstraction is presumably mediated by a nickel(I) center, which is fairly rare.<sup>8</sup>

After the generation of a methyl radical, two methylated products, the nickel acetyl species (PNP)Ni-COCH<sub>3</sub> (**2**) and the nickel methyl species (PNP)Ni-CH<sub>3</sub> (**3**), are produced. In both product formations, the five-coordinate intermediate species (PNP)Ni(CO)(CH<sub>3</sub>) (**5**) is thought to be involved. While a methyl species can be easily produced by CO elimination from the nickel(II) center of **5**, a nickel acetyl species can be generated by alkyl migration onto a CO ligand in **5**, for which the reaction is well established.<sup>14</sup> However, this

migration is unlikely to occur with **5**, since the CO insertion into a Ni–C bond in (PNP)Ni-CH<sub>3</sub> (**3**) requires a higher activation barrier. According to our experimental results obtained from the reaction of **3** with CO, the formation of the corresponding acetyl species **2** via migratory insertion requires a much longer reaction time (40 h) at room temperature, while the acyl formation from **1** with MeI takes less than 1 min under the same reaction conditions. In fact, the reaction of the corresponding zerovalent nickel carbonyl species (PNP)Ni(CO)Na with MeI, where the formation of the same five-coordinate intermediate is expected via oxidative addition, resulted in the clean formation of a nickel methyl species (**3**).<sup>6a</sup> Therefore, the possibility of another pathway is engendered, such as direct C–C bond coupling.

According to DFT calculations, the five-coordinate intermediate (PNP)Ni(CO)(CH<sub>3</sub>) (**5**) generated by Ni–C bond formation can undergo CO migratory insertion with an activation barrier of 12.8 kcal/mol (TS<sub>5Me</sub>; Figure 3). Alternatively, CO elimination occurs to generate a nickel methyl product (**3**) via a barrierless CO elimination process (TS<sub>4Me</sub>,  $\Delta G^\ddagger = < 1$  kcal/mol; Figure 3). This clearly indicates that the initial Ni–C bond formation, followed by CO elimination to produce (PNP)Ni-CH<sub>3</sub> (**3**), is energetically favorable over CO migration. In fact, the yield of **2** increases with elevated temperature, indicating that a portion of **5** overcomes the activation barrier to reveal limited, but reasonable, CO migratory insertion (Table 3). Although the contribution of **5** to the formation of **2** cannot be neglected, and interestingly the yield of **2** is always higher than that of **3**, the formation of (PNP)Ni-COCH<sub>3</sub> (**2**) might require another pathway bypassing the formation of **5**.

**Table 3.** Reaction of (PNP)Ni-CO (**1**) with MeI at Varying Temperatures

temp (°C)	yield (%)		
	Ni-I ( <b>4</b> )	Ni-COCH <sub>3</sub> ( <b>2</b> )	Ni-CH <sub>3</sub> ( <b>3</b> )
-35	50	36	14
room temp	50	39	11
60	50	41	9
100	50	43	7

DFT calculations indicate that, apart from the superior radical nature at a nickel center (67%), the rest of the spin density is distributed almost equally among the donor atoms directly coordinated to the Ni center (7% of the spin density is located on the carbon atom of a CO ligand; see the [Supporting Information](#)). Direct C–C bond formation between the carbon atom of a CO ligand and a methyl radical cannot be excluded as an alternative pathway. Due to the difficulties in modeling the biradical nature of a reacting complex and the transition state of the present system, a radical approach of **1** toward a methyl radical is modeled using the unrestricted formalism of DFT for the hypothesized reaction of **1** with MeI. Although the latter modeling certainly does not describe the desired radical–radical reaction as suggested in experiments, we believe it can at least capture the relative reactivity of the methyl species toward Ni vs carbonyl carbon. The generation of **2** occurs via a direct C–C bond formation with TS<sub>2Me</sub> ( $\Delta G^\ddagger = 16.0$  kcal/mol; [Figure 3](#)). A small methyl group can also directly couple with a nickel center to produce a five-coordinate intermediate (**5**) via TS<sub>3Me</sub> ( $\Delta G^\ddagger = 16.6$  kcal/mol; [Figure 3](#)). This intermediate (**5**) then energetically favors the formation of a nickel methyl species (**3**) rather than the C–C bond coupled product (**2**). In other words, the desired C–C bond formation may occur mainly via direct coupling, instead of involving five-coordinate species. Due to a small difference in rate-determining activation barriers for the two pathways (direct C–C coupling vs through five-coordinate intermediate species), however, the formation of both **2** and **3** seems to be quite possible to similar extents.

The reaction of free CO and alkyl radicals to form acyl radicals is considerably utilized in organic synthesis.<sup>4</sup> However, direct C–C bond formation between a coordinated CO ligand and an alkyl radical is fairly rare. Hughes and co-workers proposed direct fluoroalkylation at a CO ligand in the reaction of CpRh(PMe<sub>3</sub>)(CO) with <sup>13</sup>C<sub>3</sub>F<sub>7</sub>I, but they provided limited evidence for a radical pathway.<sup>5</sup> Goldman and co-workers proposed alkyl radical addition to d<sup>8</sup> metal carbonyls for the photocatalytic carbonylation of cyclohexane.<sup>15</sup> This system was later reevaluated theoretically, revealing that an alkyl radical directly attacks at a coordinated CO ligand, as suggested by Hasanayn and co-workers.<sup>5</sup> Our experimental and theoretical evaluations on the reaction of (PNP)Ni-CO (**1**) with alkyl iodides support that the reaction undergoes alkyl radical formation followed by its direct attack on a coordinated CO ligand. Obviously, the radical C–C bond coupling occurs at the carbon atom coordinated to a monovalent nickel ion with an even higher spin density located on a metal center.

## CONCLUSIONS

The reaction mechanism of a nickel(I) monocarbonyl species (**1**) supported by a pincer type PNP ligand with iodoalkanes was experimentally and theoretically investigated, revealing the formation of compounds **2–4**. The initial iodine radical abstraction by **1** was suggested from the increase in the yield

of a nickel(II) iodide species (**4**) when excess amount of iodoalkanes were employed. Corresponding alkyl radical generation was confirmed by trapping methyl and *tert*-butyl radicals by utilizing Gomberg's dimer. DFT calculations on the reaction of **1** with MeI suggest that the nickel-acyl formation (**2**) may not include the five-coordinate intermediate species (PNP)Ni(CO)(CH<sub>3</sub>) (**5**) but suggest direct C–C bond formation between a methyl radical and a coordinated CO ligand at a monovalent nickel center.

## EXPERIMENTAL SECTION

**General Considerations.** All manipulations were carried out using standard Schlenk or glovebox techniques under a N<sub>2</sub> atmosphere. Solvents were deoxygenated and dried by thoroughly sparging with Ar gas followed by passage through an activated alumina column. Solvents were tested with a standard purple solution of sodium benzophenone ketyl in tetrahydrofuran in order to confirm effective oxygen and moisture removal. All reagents were purchased from commercial vendors and used without further purification unless otherwise stated. (PNP)Ni-CO (**1**)<sup>6a</sup> and (CPh<sub>3</sub>)<sub>2</sub>(pentane)<sup>12b</sup> were prepared according to literature procedures. Deuterated solvents were purchased from Cambridge Isotope Laboratories, Inc., and Eurisotop, degassed, and dried over activated 4 Å molecular sieves prior to use.

**Spectroscopic Measurements.** A Bruker AVHD-400 spectrometer was used to measure <sup>1</sup>H, <sup>19</sup>F, and <sup>31</sup>P NMR spectra. <sup>13</sup>C NMR spectra were recorded on Agilent 600 spectrometers. The chemical shifts for <sup>1</sup>H NMR and <sup>13</sup>C NMR spectra are quoted in parts per million (ppm) referenced to residual solvent peaks. The chemical shifts for <sup>19</sup>F NMR spectra are referenced to external  $\alpha,\alpha,\alpha$ -trifluorotoluene as -63.72 ppm. <sup>31</sup>P NMR spectra were decoupled by broad-band proton decoupling. The chemical shifts for <sup>31</sup>P NMR spectra are quoted in parts per million (ppm) referenced to external phosphoric acid as 0.0 ppm. The following abbreviations are used to describe peak splitting patterns when appropriate: d = doublet, t = triplet, q = quartet, m = multiplet, qt = quartet of triplets. Coupling constants, *J*, are reported in hertz (Hz). The *N* values corresponding to  $(1/2)[J_{AX} + J_{AX}]$  are provided when virtual couplings are observed in the <sup>13</sup>C NMR spectra.

**Computational Details.** All of the geometries were optimized at the B3LYP/Gen1 level, where Gen1 stands for the 6-31G\* basis set for C, H, N, O, and P atoms, the 6-311G\* basis set for an I atom, and the LanL2DZ basis set for a Ni atom, as implemented in the Q-CHEM quantum chemistry package.<sup>16</sup> The radical species were treated with the spin-unrestricted formalism. The transition state searches were done using the Hessian mode following option incorporated into the Baker's eigenvector following algorithm.<sup>17</sup> Transition states (first-order saddle points) were characterized by a single imaginary frequency (negative eigenvalue for the Hessian) pertaining to the desired reaction coordinates. Energies were further refined at the B3LYP/Gen2 level, where Gen2 stands for the 6-311+G\*\* basis set for C, H, N, O, and P atoms, the 6-311G\*\* basis set for an I atom, and the LanL2DZ basis set with f polarization function for a Ni atom along with the Grimme's DFT-D3 corrections<sup>18</sup> for nonbonding interactions and single-point solvation energy correction (the solvent is THF) using the IEF-PCM method.<sup>19</sup> The discussions presented in the main text are based on the relative Gibbs energies at 298.15 K and 1 atm with respect to the infinitely separated reactants.

**Reaction of **1** with RI.** To a solution of **1** (20 mg, 0.039 mmol) in 10 mL of THF was added RI (0.040 mmol) at room temperature. The reaction mixture was stirred for 10 min, resulting in a color change from dark green to greenish yellow. Volatiles were removed under vacuum. The yields of products were determined by single-pulse <sup>31</sup>P NMR spectroscopy.

**Reaction of **1** with Excess RI.** To a solution of RI (3.90 mmol) in 5 mL of THF was added a solution of **1** (20 mg, 0.039 mmol) in 5 mL of THF dropwise at room temperature, resulting in a color change from dark green to yellow. The reaction mixture was stirred for 10

min, and volatiles were removed under vacuum. The yields of products were determined by single-pulse  $^{31}\text{P}$  NMR spectroscopy.

**Reaction of 1 with  $\text{CF}_3\text{I}$ .** A solution of 1 (10 mg, 0.019 mmol) in 5 mL of THF in a sealed Schlenk tube (total volume 17 mL) was degassed by freeze–pump–thaw cycles on a Schlenk line.  $\text{CF}_3\text{I}$  was charged under ambient conditions, resulting in an immediate color change from dark green to brown. The reaction mixture was stirred for 10 min, and volatiles were removed under vacuum. The yields of products were determined by single-pulse  $^{31}\text{P}$  NMR spectroscopy.

**Synthesis of (PNP)Ni- $\text{CF}_3$ .** To a mixture of (PNP)Ni-Cl (157 mg, 0.300 mmol) and AgF (190 mg, 1.50 mmol) in 10 mL of THF was added  $\text{Me}_3\text{SiCF}_3$  (213 mg, 1.50 mmol). The green reaction mixture was stirred for 12 h at 45 °C in the dark, resulting in a color change to red. After the volatiles were removed under vacuum, the resulting residue was dissolved in pentane. The reddish solution was filtered through Celite, and the volatiles were removed under vacuum. The resulting product (PNP)Ni- $\text{CF}_3$  (101 mg, 0.182 mmol, 60.5%) was isolated as a red solid after washing with cold pentane (–35 °C) and drying under vacuum.  $^1\text{H}$  NMR (400 MHz, benzene- $d_6$ ):  $\delta$  7.55 (d,  $J_{\text{HH}} = 8.6$  Hz, 2H), 6.93 (s, 2H), 6.76 (d,  $J_{\text{HH}} = 8.5$  Hz, 2H), 2.36–2.22 (m, 4H), 2.14 (s, 6H), 1.38 (q,  $J_{\text{HH}} = 7.7$  Hz, 12H), 1.12 (q,  $J_{\text{HH}} = 7.2$  Hz, 12H).  $^{13}\text{C}$  NMR (151 MHz, benzene- $d_6$ ):  $\delta$  161.99 (virtual t,  $N = 12.1$  Hz), 140.14 (qt,  $^1J_{\text{CF}} = 354$  Hz,  $^2J_{\text{CP}} = 31.9$  Hz), 132.58, 131.96, 125.08 (virtual t,  $N = 3.2$  Hz) 119.48 (virtual t,  $N = 20$  Hz), 116.26 (virtual t,  $N = 5.2$  Hz), 24.57 (virtual t,  $N = 11.8$  Hz), 20.55, 18.76, 17.74.  $^{19}\text{F}$  NMR (376 MHz, benzene- $d_6$ ):  $\delta$  –0.47 (t,  $^3J_{\text{FP}} = 19.9$  Hz).  $^{31}\text{P}$  NMR (162 MHz, benzene- $d_6$ ):  $\delta$  46.48 (q,  $^3J_{\text{PF}} = 19.8$  Hz). Anal. Calcd for  $\text{C}_{27}\text{H}_{40}\text{F}_3\text{NNiP}_2$ : C, 58.30; H, 7.25; N, 2.52. Found: C, 58.53; H, 7.29; N, 2.33. UV–vis [THF, nm (L mol $^{-1}$  cm $^{-1}$ )]: 504 (568), ~392 (sh, 2500), 340 (16100), 337 (17200), 333 (15300), 314 (10300).

**Reaction of 1 with RI in the Presence of Gomberg's Dimer.** To a mixture of 1 (20 mg, 0.039 mmol) and  $(\text{CPh}_3)_2$  (pentane) (0.019 or 0.194 mmol) in 10 mL of THF was added RI (0.040 mmol) at room temperature (or –35 °C). The reaction mixture was stirred for 10 min (12 h for –35 °C), resulting in a color change from dark green to greenish yellow. Volatiles were removed under vacuum. The yields of products were determined by single-pulse  $^{31}\text{P}$  NMR spectroscopy.

**Synthesis of  $\text{Ph}_3\text{C}^t\text{Bu}$ .** To a mixture of 1 (50 mg, 0.097 mmol) and  $(\text{CPh}_3)_2$  (pentane) (27 mg, 0.048 mmol) in 10 mL of THF was added  $^t\text{BuI}$  (12  $\mu\text{L}$ , 18 mg, 0.040 mmol) at room temperature. The reaction mixture was stirred for 10 min, resulting in a color change from dark green to greenish yellow. Volatiles were removed under vacuum.  $\text{Ph}_3\text{C}^t\text{Bu}$  (11 mg, 0.037 mmol, 38%) was obtained as a white solid after purification via silica gel column chromatography using EA/hexane 1/40 v/v as eluent.

**Synthesis of  $\text{Ph}_3\text{CMe}$ .** Author: To a mixture of 1 (50 mg, 0.097 mmol) and  $(\text{CPh}_3)_2$  (pentane) (271 mg, 0.485 mmol) in 10 mL of THF was added MeI (50  $\mu\text{L}$ , 2.0 M solution in  $^t\text{BuOMe}$ , 0.10 mmol) at room temperature. The reaction mixture was stirred for 10 min, resulting in a color change from dark green to greenish yellow. Volatiles were removed under vacuum.  $\text{Ph}_3\text{CMe}$  (8.1 mg, 0.031 mmol, 32%) was obtained as a white solid after purification by silica gel column chromatography using EA/hexane 1/40 v/v as eluent.

**Reaction of 1 with MeI at Varying Temperatures.** To a solution of 1 (20 mg, 0.039 mmol) in 10 mL of toluene was added MeI (20  $\mu\text{L}$ , 2.0 M solution in  $^t\text{BuOMe}$ , 0.040 mmol) at different temperatures (–35, 25, 60, and 100 °C). The reaction mixture was stirred for 10 min (12 h for –35 °C), and volatiles were removed under vacuum. The yields of products were determined by single-pulse  $^{31}\text{P}$  NMR spectroscopy.

## ■ ASSOCIATED CONTENT

### Supporting Information

The Supporting Information is available free of charge on the ACS Publications website at DOI: 10.1021/acs.organo- met.5b00548.

NMR spectra, X-ray crystallographic data for (PNP)Ni- $\text{CF}_3$ , and details of DFT calculations (PDF)  
X-ray crystallographic data for (PNP)Ni- $\text{CF}_3$  (CIF)  
Cartesian coordinates for calculated structures (XYZ)

## ■ AUTHOR INFORMATION

### Corresponding Authors

\*E-mail for Y.J.: ysjn@kaist.ac.kr.

\*E-mail for Y.L.: yunholee@kaist.ac.kr.

### Notes

The authors declare no competing financial interest.

## ■ ACKNOWLEDGMENTS

This work has been financially supported by KAIST and Aramco Overseas Company.

## ■ REFERENCES

- (1) Tasker, S. Z.; Standley, E. A.; Jamison, T. F. *Nature* **2014**, *509*, 299–309.
- (2) Reviews of nickel(I) in cross-coupling reactions: (a) Han, F.-S. *Chem. Soc. Rev.* **2013**, *42*, 5270–5298. (b) Hu, X. *Chem. Sci.* **2011**, *2*, 1867–1886. (c) Phapale, V. B.; Cárdenas, D. J. *Chem. Soc. Rev.* **2009**, *38*, 1598–1607.
- (3) (a) Can, M.; Armstrong, F. A.; Ragsdale, S. W. *Chem. Rev.* **2014**, *114*, 4149–4174. (b) Bender, G.; Stich, T. A.; Yan, L.; Britt, R. D.; Cramer, S. P.; Ragsdale, S. W. *Biochemistry* **2010**, *49*, 7516–7523.
- (4) (a) Sumino, S.; Fusano, A.; Fukuyama, T.; Ryu, I. *Acc. Chem. Res.* **2014**, *47*, 1563–1574. (b) Ryu, I.; Sonoda, N. *Angew. Chem., Int. Ed. Engl.* **1996**, *35*, 1050–1066.
- (5) Hasanayn, F.; Nsouli, N. H.; Al-Ayoubi, A.; Goldman, A. S. *J. Am. Chem. Soc.* **2008**, *130*, 511–521.
- (6) (a) Yoo, C.; Oh, S.; Kim, J.; Lee, Y. *Chem. Sci.* **2014**, *5*, 3853–3858. (b) Yoo, C.; Kim, J.; Lee, Y. *Organometallics* **2013**, *32*, 7195–7203.
- (7) (a) Schley, N. D.; Fu, G. C. *J. Am. Chem. Soc.* **2014**, *136*, 16588–16593. (b) Lin, X.; Phillips, D. L. *J. Org. Chem.* **2008**, *73*, 3680–3688. (c) Phapale, V. B.; Buñuel, E.; Garcia-Iglesias, M.; Cárdenas, D. J. *Angew. Chem., Int. Ed.* **2007**, *46*, 8790–8795. (d) Jones, G. D.; Martin, J. L.; McFarland, C.; Allen, O. R.; Hall, R. E.; Haley, A. D.; Brandon, R. J.; Konovalova, T.; Desrochers, P. J.; Pulay, P.; Vicio, D. A. *J. Am. Chem. Soc.* **2006**, *128*, 13175–13183. (e) Anderson, T. J.; Jones, G. D.; Vicio, D. A. *J. Am. Chem. Soc.* **2004**, *126*, 8100–8101.
- (8) (a) Laskowski, C. A.; Bungum, D. J.; Baldwin, S. M.; Del Ciello, S. A.; Iluc, V. M.; Hillhouse, G. L. *J. Am. Chem. Soc.* **2013**, *135*, 18272–18275. (b) Marlier, E. E.; Tereniak, S. J.; Ding, K.; Mulliken, J. E.; Lu, C. C. *Inorg. Chem.* **2011**, *50*, 9290–9299.
- (9) (a) Yuan, J.; Hughes, R. P.; Rheingold, A. L. *Organometallics* **2011**, *30*, 1744–1746. (b) Bourgeois, C. J.; Hughes, R. P.; Husebo, T. L.; Smith, J. M.; Guzei, I. M.; Liable-Sands, L. M.; Zakharov, L. N.; Rheingold, A. L. *Organometallics* **2005**, *24*, 6431–6439.
- (10) Product yields were determined by relative determination of peak areas found in single-pulse  $^{31}\text{P}$  NMR spectra. Other potential organic products were not evaluated.
- (11) Three products were obtained from the reaction of (PNP)Ni-CO (1) with  $\text{CF}_3\text{I}$ . The formation of (PNP)Ni-I (64%) and (PNP)Ni- $\text{CF}_3$  (19%) was confirmed by comparing their  $^{31}\text{P}$  NMR data. The other product (18%) displaying a  $^{31}\text{P}$  NMR signal at 42.13 ppm is assigned as (PNP)Ni-COCF $_3$  (see the Supporting Information). Independently, (PNP)Ni- $\text{CF}_3$  was synthesized and characterized (see the Experimental Section).
- (12) (a) Gomberg, M. *J. Am. Chem. Soc.* **1900**, *22*, 757–771. (b) Jang, E. S.; McMullin, C. L.; Käß, M.; Meyer, K.; Cundari, T. R.; Warren, T. H. *J. Am. Chem. Soc.* **2014**, *136*, 10930–10940.
- (13) Hush, N. S.; Oldham, K. B. *J. Electroanal. Chem.* **1963**, *6*, 34–45.
- (14) Cavell, K. J. *Coord. Chem. Rev.* **1996**, *155*, 209–243.

(15) (a) Boese, W. T.; Goldman, A. S. *J. Am. Chem. Soc.* **1992**, *114*, 350–351. (b) Boese, W. T.; Goldman, A. S. *Tetrahedron Lett.* **1992**, *33*, 2119–2122.

(16) Shao, Y.; Molnar, L. F.; Jung, Y.; Kussmann, J.; Ochsenfeld, C.; Brown, S. T.; Gilbert, A. T. B.; Slipchenko, L. V.; Levchenko, S. V.; O'Neill, D. P.; DiStasio, R. A., Jr; Lochan, R. C.; Wang, T.; Beran, G. J. O.; Besley, N. A.; Herbert, J. M.; Lin, C. Y.; Van Voorhis, T.; Chien, S. H.; Sodt, A.; Steele, R. P.; Rassolov, V. A.; Maslen, P. E.; Korambath, P. P.; Adamson, R. D.; Austin, B.; Baker, J.; Byrd, E. F. C.; Dachsel, H.; Doerksen, R. J.; Dreuw, A.; Dunietz, B. D.; Dutoi, A. D.; Furlani, T. R.; Gwaltney, S. R.; Heyden, A.; Hirata, S.; Hsu, C.-P.; Kedziora, G.; Khalliulin, R. Z.; Klunzinger, P.; Lee, A. M.; Lee, M. S.; Liang, W.; Lotan, I.; Nair, N.; Peters, B.; Proynov, E. I.; Pieniazek, P. A.; Rhee, Y. M.; Ritchie, J.; Rosta, E.; Sherrill, C. D.; Simmonett, A. C.; Subotnik, J. E.; Woodcock, H. L., III; Zhang, W.; Bell, A. T.; Chakraborty, A. K.; Chipman, D. M.; Keil, F. J.; Warshel, A.; Hehre, W. J.; Schaefer, H. F., III; Kong, J.; Krylov, A. L.; Gill, P. M. W.; Head-Gordon, M. *Phys. Chem. Chem. Phys.* **2006**, *8*, 3172–3191.

(17) Baker, J. J. *Comput. Chem.* **1997**, *18*, 1079–1095.

(18) (a) Grimme, S.; Antony, J.; Ehrlich, S.; Krieg, H. *J. Chem. Phys.* **2010**, *132*, 154104–154119. (b) Grimme, S.; Ehrlich, S.; Goerigk, L. *J. Comput. Chem.* **2011**, *32*, 1456–1465.

(19) (a) Barone, V.; Cossi, M.; Tomasi, J. *J. Chem. Phys.* **1997**, *107*, 3210–3221. (b) Mennucci, B.; Cammi, R.; Tomasi, J. *J. Chem. Phys.* **1999**, *110*, 6858–6870.